Strål
säkerhets
myndigheten
Swedish Radiation Safety Authority

Authors: Goodluck I. Ofoegbu
Kevin J. Smart

Technical Note

2013:35

Rock Mechanics – Confidence of SKB's models for predicting the occurrence of a damage zone around the excavations

Main Review Phase

Report number: 2013:35 **ISSN:** 2000-0456
Available at www.stralsakerhetsmyndigheten.se

SSM perspektiv

Bakgrund

Strålsäkerhetsmyndigheten (SSM) granskar Svensk Kärnbränslehantering AB:s (SKB) ansökningar enligt lagen (1984:3) om kärnteknisk verksamhet om uppförande, innehav och drift av ett slutförvar för använt kärnbränsle och av en inkapslingsanläggning. Som en del i granskningen ger SSM konsulter uppdrag för att inhämta information och göra expertbedömningar i avgränsade frågor. I SSM:s Technical Note-serie rapporteras resultaten från dessa konsultuppdrag.

Projektets syfte

Det övergripande syftet med projektet är att ta fram synpunkter på SKB:s säkerhetsanalys SR-Site för den långsiktiga strålsäkerheten hos det planerade slutförvaret i Forsmark. Konsulterna har utvärderat tilltron till SKB:s modeller för att bedöma utbredningen av bergskador kring ett bergutrymme i slutförvaret. Utvärderingen har genomförts med hänsyn till SKB:s osäkerheter på den konceptuella modellen, bergspänningsfältet, bergmaterialparametrarna samt effekten av schaktningsmetoden. Oberoende modellering av bergskadezonen har också genomförts för att simulera initialtillståndet samt den långsiktiga utvecklingen av slutförvaret.

Författarnas sammanfattning

Detta konsultuppdrag, genomfört av Southwest Research Institute, fokuserar på en utvärdering av SKB:s analyser av förekomsten av bergskadezonen (Excavation Damage Zone, EDZ) runtom bergutrymmen i slutförvaret. Rapporten redovisar konsulternas vetenskapliga bedömning av SKB:s analyser inom detta område utifrån SSM ställda frågor. Bedömningen innefattar oberoende beräkningar som konsulterna har genomfört med alternativ modell och programvara för att utvärdera förekomsten av EDZ samt dess spatiala utbredning. De oberoende beräkningarna tar hänsyn till spänningseffekter på grund av schaktning, termiska och glaciala laster, grundvattentryck samt bentonitsvällstryck.

Även SKB har analyserat bergskadezonen i samband med utschaktning på grund av spänningskoncentrationer, laster under den termala samt glaciala fasen inklusive effekten av grundvattentrycket. Baserat på dessa analyser har SKB inkluderat en EDZ med tjocklek på 30 cm under deponeringstunnelssulan för att studera dess effekt på radionuklidtransport i närområdet. SKB tilldelar EDZ en transmissivitet på 10-8 m2/s parallellt med deponeringstunnlarna. SKB inkluderar inte någon skadezon för deponeringshålen men tar hänsyn till bergskador på grund av spjälkning av berget som påverkar flödesvägarna i deponeringshålens väggar.

Konsulterna bedömde grunderna för SKB:s hantering av bergskadezonen för modellering av vattenströmning och radionuklidtransport samt studerade möjligheten att vissa konfigurationer av EDZ inte var inkluderade i SKB:s redovisning. Konsulterna konstaterade att SKB:s hantering av bergskadezonen under schaktning av bergutrymmen överensstämmer med antagna schaktningstekniker. Konsulterna genomförde oberoende

modellering för att bedöma effekten av berg- och bergmassans hållfasthet, belastningsfall samt riktningen på deponeringstunnlarna i förhållande till riktningen för den ursprungliga maximala horisontella huvudspänningen. Beräkningarna indikerar att SKB:s antagande av EDZ i närområdet överensstämmer med dagens förståelse för de aktuella bergmekaniska förhållandena samt framtida belastningsfall gällande dimensioneringen av slutförvaret i Forsmark (SSM:s anm.: d.v.s. ingen förekomst av kontinuerlig EDZ), om den maximala riktningsskillnaden mellan den ursprungliga maximala huvudspänningen och deponeringstunnlarna är begränsad (konsulternas beräkningar uppskattar att 22.5˚ inte skulle vara för stort). Emellertid, om den maximala riktningsskillnaden är stor (konsulternas beräkningar uppskattar att 45˚ skulle vara tillräckligt stort), då bör SKB:s antagande av EDZ i närområdet anpassas för att ta hänsyn till en spänningsinducerad bergskadezon (SSM:s anm.: d.v.s. förekomst av kontinuerlig EDZ).

Projektinformation
Kontaktperson på SSM: Flavio Lanaro
Diarienummer ramavtal: SSM2011-3639
Diarienummer avrop: SSM2013-2462
Aktivitetsnummer: 3030012-4060

SSM perspective

Background

The Swedish Radiation Safety Authority (SSM) reviews the Swedish Nuclear Fuel Company's (SKB) applications under the Act on Nuclear Activities (SFS 1984:3) for the construction and operation of a repository for spent nuclear fuel and for an encapsulation facility. As part of the review, SSM commissions consultants to carry out work in order to obtain information and provide expert opinion on specific issues. The results from the consultants' tasks are reported in SSM's Technical Note series.

Objectives of the project

The general objective of the project is to provide review comments on SKB's post-closure safety analysis, SR-Site, for the proposed repository at Forsmark. The consultants have evaluated the confidence that can be placed in SKB's models for predicting the occurrence of a damage zone in the rock around the excavations. The evaluation was done based on SKB's uncertainties on the conceptual models, rock stresses and material properties, and on the effects of the chosen excavation methods for deposition tunnels and holes in the rock at Forsmark. Independent modelling of a damaged zone was carried out for the initial conditions and long-term behavior of the repository.

Summary by the authors

This assignment, performed at Southwest Research Institute, focusses on evaluating SKB's assessment of potential occurrence of damaged rock zones (also referred to as excavation-damaged zone or EDZ) around underground excavations at the site. This report presents the authors' evaluation of SKB's assessment in the specific area based on questions raised by SSM. The evaluation includes independent calculations by the authors using alternative models and codes to assess potential EDZ configurations and spatial persistence. The independent calculations consider the effects of stress change due to excavation, thermal and glacial loadings, buffer swelling and groundwater pressure.

SKB assessed potential EDZ occurrence due to construction and the stress effects of excavation, thermal loading, glacially induced loading and pore pressure. Based on the assessment, SKB, in its modelling of near-field flow and radionuclide transport, includes a 30-cm thick EDZ at the floor of the deposition tunnel. SKB assigns the EDZ a tunnel-parallel transmissivity of 10-8 m2/s to assess potential effects of rock damage on safety functions. For deposition holes, SKB does not include an explicit EDZ but accounts for potential damage due to spalling by modifying the flow pathways at the wall of the deposition hole.

The authors evaluated the basis for the SKB representation of EDZ in flow and transport modelling and assessed potential occurrence of EDZ configurations not encompassed by the SKB representation. The authors concluded that the SKB assessment of potential EDZ due to construction alone is consistent with the excavation techniques presented by SKB. The

authors performed independent calculations to examine the effects of rock strength modelling, loading conditions and the deposition-tunnel orientation relative to the maximum in situ horizontal stress. The authors' calculations indicate that the SKB representation of potential EDZ in near-field flow and transport modelling would be consistent with the current understanding of rock mechanics and loading conditions for underground design of the repository at Forsmark (Editor's note: no occurrence of continuous EDZ), if the maximum deviation of the deposition tunnel orientation from the direction of the maximum in situ horizontal stress is held within a small limit (the authors' calculations indicate that a 22.5° deviation would not be too large). However, if the tunnel layout includes the possibility for a large deviation of the tunnel orientation from the direction of the maximum horizontal stress (the authors' independent analysis indicates that a 45° deviation would be large enough), then the EDZ configuration would need to be modified to account for potential stress-induced rock damage (Editor's note: occurrence of continuous EDZ).

Project information
Contact person at SSM: Flavio Lanaro

Strål
säkerhets
myndigheten
Swedish Radiation Safety Authority

Authors: Goodluck I. Ofoegbu and Kevin J. Smart
Southwest Research Institute, San Antonio, Texas, USA

Technical Note 43

2013:35

Rock Mechanics – Confidence of SKB's models for predicting the occurrence of a damage zone around the excavations

Main Review Phase

Date: September 2013
Report number: 2013:35 **ISSN:** 2000-0456
Available at www.stralsakerhetsmyndigheten.se

This report was commissioned by the Swedish Radiation Safety Authority (SSM). The conclusions and viewpoints presented in the report are those of the author(s) and do not necessarily coincide with those of SSM.

Contents

1. Introduction

This assignment is part of the Swedish Radiation Safety Authority (SSM) Main Review Phase of the SR-Site safety assessment provided by the Swedish Nuclear Fuel and Waste Management Company (SKB) for final disposal of spent nuclear fuel at the Forsmark site. Based on the Initial Review Phase of SSM's review of SR-Site, SSM concluded that SKB's reporting is sufficiently comprehensive and of sufficient quality to justify a continuation to the Main Review Phase. The Main Review Phase is targeted at tasks and issues prioritized by SSM with the intention to indirectly or directly support SSM's compliance judgments. The review includes detailed analysis of a range of specific issues for which SSM has judged that further input from SSM's external experts will be helpful. Each assignment to SSM's external experts will include a definition of one or several specific issues or areas that require detailed assessment.

The current assignment to Southwest Research Institute® focuses on evaluating the confidence that can be placed in SKB's models for predicting the occurrence of a damage zone in the rock around the repository excavations. The evaluation is based on SKB's uncertainties in the conceptual models, rock stresses, and material properties, and on the effects of the chosen excavation methods for deposition tunnels and deposition holes in the rock at Forsmark. This report presents the authors' evaluation of SKB's assessment in the specific area based on questions raised by SSM. Parts of the evaluation are supported using independent confirmatory calculations performed by the authors.

2. Damage zone around the excavations

This assignment consists of evaluating SKB's assessment of the potential occurrence of damaged rock zones (also referred to as excavation-damaged zones or EDZs) around the excavations. The evaluation focuses on the definition of potential EDZ configurations around the deposition holes and tunnels, contributions of construction-induced and stress-induced rock damage to the EDZ, and possible mitigation of EDZ effects prior to waste emplacement. The evaluation includes independent calculations by the authors using alternative models and codes to assess potential EDZ configurations and spatial persistence against SKB's modelling. The independent calculations consider the effects of stress change due to excavation, thermal and glacial loadings, and groundwater pressure. The calculation results are used to support an evaluation of whether the current level of uncertainty regarding EDZ occurrence and the rock stresses and their long-term evolution can be considered acceptable, allowing the repository application to proceed to the construction phase.

2.1. SKB's presentation

SKB (2011) assessed potential rock damage (i.e., formation of new fractures or slip or opening of existing fractures) within the near-field zone of the deposition tunnel and deposition hole to estimate values of rock-mass hydraulic conductivity applicable to modelling near-field water flow and radionuclide transport. Rock damage could cause the applicable hydraulic conductivity to increase. SKB (2010a) established that the effective transmissivity for water flow parallel to a deposition hole through a connected damage zone along the full length of the deposition hole should be smaller than 10^{-10} m^2/s. Also, according to SKB (2010a), the effective transmissivity for water flow parallel to a deposition tunnel through a connected damage zone at least 20–30 m long at the tunnel floor should be no greater than 10^{-8} m^2/s. SKB assessed the potential for rock damage resulting from construction and stress change due to excavation, thermal loading, and glacier-induced loading and pore pressure. Based on the assessment, SKB (2011, p. 348–349) concluded that a damage zone with tunnel-parallel transmissivity of 10^{-8} m^2/s needs to be included in the near-field transport model and used to further assess the potential effects of rock damage on safety functions. For deposition holes, SKB does not include an explicit EDZ but accounts for potential damage due to spalling by modifying the flow rate to a stylized horizontal fracture that intersects the deposition hole (SKB, 2011, p. 349). The bases for the SKB conclusions are discussed in the following sections.

2.1.1. Rock damage around deposition holes

To assess the potential for construction-induced damage around deposition holes, SKB (2011, p. 294) relied on a literature review by Bäckblom (2008) to conclude that the chosen construction method of full face down-hole drilling for deposition holes will result in negligible rock damage. According to SKB, if deposition-hole construction were to result in damage to the surrounding rock, the depth of damaged rock from the wall will not exceed a few centimeters and the damage zone transmissivity parallel to the hole will be smaller than the design premise value of 10^{-10} m^2/s. Also, according to SKB (2011, p. 153–154), deposition holes in tunnels

aligned at an angle greater than 30° from the maximum horizontal *in situ* stress direction could sustain damage due to spalling (rock plates and shards breaking and detaching from the rock wall), because SKB analyses described in the SR-Site main report (SKB, 2011, p. 294) indicate that stress concentration due to the deposition hole could exceed the spalling strength of the rock. If the deposition tunnel alignments are within 0°–30° from the maximum horizontal *in situ* stress direction, approximately 100–200 deposition holes out of 6,000 would sustain an overbreak of 5 cm or more due to spalling (SKB, 2011, p. 154). To keep potential spalling damage of deposition holes within these limits, SKB (2011, p. 154) stated that the deposition tunnels in the reference design are aligned between azimuths 123 and 140°. The maximum horizontal *in situ* stress direction is 145±15°, according to the SR-Site data report (SKB, 2010b, p. 277).

SKB (2011, p. 294) stated that spalling of the deposition hole wall before waste emplacement does not present a concern for repository safety because any loose rock debris will be removed and large overbreaks filled with buffer material prior to waste emplacement. Also, according to SKB (2011, p. 294), a deposition hole could be rejected if damage to the wall rock could not be repaired as envisaged in the underground openings construction report (SKB, 2010a).

According to SKB (2011, p. 335–336), additional spalling of the deposition hole wall could occur during the thermal period after closure of the deposition holes and tunnels, because SKB analyses indicate that the increased stress on the wall will likely exceed the spalling strength of the rock in all deposition holes. However, SKB (2011, p. 335) stated that the indication of potential spalling during this period is inconclusive because the swelling pressure in the bentonite buffer will likely reduce the potential for spalling but was not accounted for in the analyses. Based on the analyses results, SKB (2011, p. 335) stated that it will assume that thermally induced spalling of the deposition hole is likely and needs to be considered in assessing flow and transport across the rock-buffer interface.

2.1.2. Rock damage around deposition tunnels

To assess the potential for construction-induced damage around deposition tunnels, SKB (2011, p. 159–160 and 295–296) used: (a) a review of previous experiments and studies in Canada, Finland, Japan, Sweden and Switzerland (Bäckblom, 2008); (b) experience gained from the TASQ tunnel excavated at the Äspö Hard Rock Laboratory (Olsson et al., 2004); and (c) studies of construction-induced damage resulting from using smooth-blasting techniques to excavate the TASS tunnel at the Äspö Hard Rock Laboratory (Olsson et al., 2009; Ericsson et al., 2009). Based on information from these studies, SKB (2011, p. 159–160 and 295–296) concluded that: (i) careful control of excavation techniques can reduce the occurrence of construction-induced damage, (ii) using smooth blasting techniques to excavate the deposition tunnels will likely result in blast-induced fractures that are dominantly radial and fracture zones that are not continuous over any significant distance along the axial direction of the tunnel, and (iii) the hydraulic conductivity within a blast-induced fracture zone is on the order of 10^{-8} m/s.

According to SKB (2011, p. 160), if stress-induced damage such as spalling occurs in addition to the construction-induced damage, the damage zone could extend tens of centimeters into the surrounding rock and the hydraulic conductivity of the zone will be on the order of 10^{-6} m/s based on the experiments reviewed by Bäckblom (2008).

SKB concluded in the SR-Site main report (SKB, 2011, p. 160) that the likelihood that there will be no axially continuous damage zone could be judged, but there is no reliable direct method to quantify the connected effective transmissivity for representing the effect of rock damage around the tunnel. Therefore, SKB (2011, p. 160) stated that its approach for controlling and accounting for rock damage around the deposition tunnels consists of the following: (i) develop and implement procedures to control and inspect the drilling, charging, and ignition sequences and include the procedures in the monitoring and control programs for the underground openings; (ii) evaluate the effects of rock conditions on rock damage within the framework of the observational method and the associated monitoring program by combining results from geological characterization, geophysical techniques, and geological modelling; and (iii) reduce the likelihood of stress-induced damage such as spalling by aligning the deposition tunnels approximately parallel to the direction of the maximum principal horizontal stress. To account for the potential effects of rock damage around the deposition tunnels, SKB (2011, p. 348) includes in the near-field flow and transport model an EDZ with a transmissivity of 10^{-8} m^2/s and thickness of 0.3 m at the tunnel floor. SKB (2011, p. 348) described the flow and transport model with the EDZ as a basic assumption for further analyses and has used the model to show that the Q2 flux (SKB, 2011, Figure 13-13) is sensitive to the EDZ transmissivity.

2.1.3. Reactivation of fractures due to stress change

SKB (2011, p. 333–335 and 459–462) assessed potential reactivation of fractures due to stress change and the effects of such reactivation on fracture transmissivity using analyses by Hökmark et al. (2010). The analyses considered stress change due to thermal and glacial loading and groundwater pressure and were based on modelling the rock mass as an assemblage of linear elastic rock blocks and discrete fractures (SKB, 2011, Figure 10-18, p. 330–336). In the analyses, the calculated stress change was interpreted using a prescribed stress-transmissivity model to estimate the potential change in transmissivity of stylized fractures (i.e., planar fractures of given orientations at selected depths). Based on the analyses, SKB (2011, p. 334, 335, 460, and 462) concluded that the effect of fracture reactivation on transmissivity is negligible and need not be included in hydrological modelling.

2.2. Motivation of the assessment

Zones of "damaged rock" could occur around underground excavations and could result from the effects of construction or stress change due to excavation or internal and external loading. The damaged rock zone, referred to as the EDZ, could be important because the damaged-rock permeability is enhanced relative to the permeability of the undamaged rock. Consequently, the EDZ could affect groundwater flow and radionuclide transport. The EDZ geometry (i.e., size and shape) and permeability enhancement need to be characterized to estimate potential effects on flow and transport. In its SR-Site analysis for a repository at the Forsmark site, SKB used a flow and transport model that includes three stylized flow paths: (i) a flow path Q1 representing a horizontal fracture that intersects a deposition hole, (ii) a second flow path Q2 representing an EDZ at the floor of and below the deposition tunnel, and (iii) a third flow path Q3 representing a fracture that intersects the deposition tunnel (SKB, 2011, p. 648). According to SKB, the flux input to Q1 will be modified to account for spalling of the deposition hole (SKB, 2011, p. 349)

and the Q2 flux will be based on a 0.3-m-thick EDZ with a transmissivity of 10^{-8} m^2/s (SKB, 2011, p. 348).

The purpose of this assessment is to evaluate the basis for the SKB representation of EDZ in flow and transport modelling and determine the potential occurrence of EDZ configurations not encompassed by the SKB representation. For example, the potential occurrence of a vertically persistent EDZ around the deposition hole will be evaluated. If the stress conditions in the host rock as modified due to excavation, thermal loading, groundwater pressure evolution, and glacial loading would tend to exceed the rock strength, then inelastic deformation of the rock could occur and could be accommodated by rock fracturing or movement on existing fractures. Such deformation, if it were to occur, could result in more extensive and connected EDZ than would result from construction effects alone. Also, such inelastic deformation, if it were to occur, could extend into the rock beyond the zone affected by spalling and would be more likely than spalling alone to form an axially connected EDZ around the deposition hole and tunnel. An axially connected EDZ around a deposition hole could result in increased fluxes for the Q1 and Q2 stylized flow paths. Also, the transmissivity for Q2 could increase considerably if the EDZ were to extend deeper below the tunnel floor or higher around the tunnel above the floor.

The authors performed independent analyses to assess the mechanical conditions around the deposition tunnels and holes to determine the potential occurrence of inelastic deformation. The analyses focussed on evaluating potential occurrence of inelastic deformation in the host rock interior surrounding the disposal excavations. Such analysis differs from spalling analysis, which assesses the potential for rock plates and shards breaking off the wall of an excavation. The constitutive models used for spalling analysis (e.g., Diederichs, 2007) are not applicable for modelling the mechanical response within the interior of a rock mass. Spalling occurs under conditions of zero or near-zero confinement and appears governed by a rock strength that is much smaller than the strength predicted using a pressure-dependent failure criterion such as the Mohr-Coulomb or Hoek-Brown criterion (e.g., Diederichs, 2007). In contrast, mechanical response within a rock mass interior is best represented using a constitutive model that includes pressure-dependent strength and dilation criteria, especially for hard crystalline rock such as the proposed repository host at the Forsmark site that shows a high rate of strength increase in relation to confinement. The Mohr-Coulomb strength criterion provides for describing rock strength and dilation as functions of confinement in a generalized elastic-plastic formulation to determine potential occurrence of brittle inelastic deformation. The model has been used widely in rock mechanics and structural geology and has been shown to lead to calculated behaviour that is consistent with documented rock mass deformation phenomena (e.g. Ord, 1991).

For the analyses, the authors considered the initial *in situ* stress, stress changes due to excavation, thermal load, groundwater pressure, and glacial loading based on SKB data and uncertainties as described in Section 2.3.2 and Appendix 2. The authors assessed the effects of such uncertainties on rock damage prediction but did not evaluate the SKB characterization of the uncertainties because such evaluation would have been beyond the scope of the assignment. The authors considered the SKB characterization of rock stress and material properties as input for the analysis to evaluate the SKB rock damage assessment. The results of the analyses are discussed in the following section.

2.3. The Consultants' assessment

The authors' evaluation of SKB information (listed in Appendix 1) regarding potential EDZ configurations due to construction and stress change is presented in this section.

2.3.1. Construction-induced damage

SKB information on the deposition holes was that rock damage due to construction will be insignificant and need not be considered in further analysis. For the deposition tunnels, SKB information was that an axially continuous and 0.3-m-thick EDZ at the base of the tunnel is sufficient to represent potential rock damage due to construction. The authors' evaluation of this information is presented in this section.

Damage around deposition holes due to construction

The SKB assessment of the potential for construction-induced damage around deposition holes was based on a review of previous studies, including full-scale experiments (Bäckblom, 2008), that showed that full face down-hole drilling in crystalline rock will likely result in negligible rock damage. Bäckblom (2008) reviewed information from construction using a Tunnel Boring Machine at Äspö Hard Rock Laboratory and at Grimsel in Switzerland that resulted in a damage zone smaller than 5 mm thick with a hydraulic conductivity of about 10^{-9} m/s. Therefore, the authors conclude that the information provided by SKB supports the conclusion that excavation of the deposition holes at the Forsmark site using full-face mechanical drilling will likely result in negligible damage to the surrounding rock.

Damage around deposition tunnels due to construction

The SKB assessment of the potential for construction-induced damage around deposition tunnels was based on a review of well-documented field experiments at crystalline rock sites similar to the Forsmark site. Results of the experiments support SKB's conclusion that rock damage due to tunnel construction can be reduced through careful control of excavation techniques. Also, the studies indicate that using smooth blasting techniques to excavate the deposition tunnels as SKB discussed will likely result in blast-induced fractures that are dominantly radial and fracture zones that are not continuous over any significant distance along the axial direction of the tunnel. SKB will develop and implement procedures to control and inspect the drilling, charging, and ignition sequences and include the procedures in the monitoring and control programs for the underground openings to ensure reliable implementation of the smooth blasting technique. However, because there is no reliable direct method to quantify the connected effective transmissivity of an EDZ, SKB included a 0.3-m-thick EDZ at the base of the deposition tunnel in the flow and transport model to represent potential rock damage due to construction and stress change. The authors conclude that the information provided by SKB supports using such an EDZ configuration to represent construction effects.

2.3.2. Rock damage due to stress changes

For the deposition holes, SKB represented rock damage due to spalling by modifying the flux input into the Q1 stylized flow path but did not provide an assessment of potential stress-induced damage by other mechanisms. For deposition

tunnels, SKB assumed that the 0.3-m-thick EDZ at the base of the tunnel is sufficient to represent potential rock damage due to construction and stress change. The authors performed independent calculations to evaluate the SKB information.

The authors used a geometrical model of the deposition area, which they modified to examine various models of the rock strength, loading conditions, and deposition-tunnel orientation relative to the maximum horizontal principal compressive stress. They performed the calculations using the finite element code ABAQUS with a built-in elastic-plastic constitutive model based on linear elasticity and the Mohr-Coulomb yield criteria (Dassault Systèmes, 2012). The modelled loadings include the *in situ* stress modified by excavation, temperature history from a waste canister, groundwater pressure, swelling pressure in the buffer and backfill, and stress and pore pressure change due to glacial loading. The buffer (in the deposition hole) and backfill (in the deposition tunnel) were not modelled explicitly, but the swelling pressure was represented as a boundary pressure on the rock wall of the opening using information from SKB (2011, p. 373–379). The groundwater pressure was specified based on the site hydraulic gradient and, along with the swelling pressure, was phased in according to saturation time determined based on information from SKB (2011, p. 368–373). Stress change due to glacial loading and the associated groundwater pressure were based on SKB (2011, p. 458–459).

The purpose of the analysis was to predict inelastic deformation if the stress conditions permitted such deformation. The authors interpreted the inelastic deformation as indicating stress-induced rock damage, because, in a hard crystalline rock such as the deposition area host rock at the Forsmark site, inelastic deformation would be accommodated through combinations of new fracturing and movement on existing fractures. However, there is currently no known numerical correspondence between inelastic strain and fracturing that would enable a quantification of the calculated inelastic strain in terms of damage intensity. The authors interpreted the zone of non-zero inelastic strain as representing the zone of damaged or fractured rock. The models and calculated results are described in Appendix 2 and summarized in Table 1.

As Table 1 shows, the calculations performed using the intact rock properties to model the mechanical behaviour of the host rock did not result in inelastic deformation anywhere (models 1–3). For model 2, the authors used the minimum tensile strength (7.9 MPa) in combination with mean values for other intact rock properties. For model 3, the authors used the minimum tensile strength and maximum Young's modulus (78 GPa) with mean values for the other intact rock properties. Using the minimum tensile strength enabled the authors to explore tension triggering of inelastic deformation. Also, using the maximum Young's modulus enabled the authors to maximize the thermally induced stress. However, none of these combinations satisfied the condition for inelastic deformation at any point in the model.

Another set of calculations was performed using the rock mass properties to model the mechanical behaviour of the host rock (models 4–8).
The authors used models 4–7 to explore the effects of loading conditions anticipated to operate during the initial temperate period (repository closure to ~10,000 years). Loadings due to the *in situ* stress modified by excavation, heat from the emplaced waste, groundwater pressure, and the swelling pressure of buffer and backfill are anticipated to operate during this period. The authors used model 8 to explore the effects of glacial loading and pore pressure anticipated to occur during subsequent glacial cycles. Model 8 used the same material properties and loading conditions as

model 5, but differed from model 5 by the addition of a cycle of glacial loading starting at 50,000 years.

As Table 1 shows, the loading combinations during the initial temperate period and subsequent glacial loading are not likely to result in inelastic deformation of the rock if the deposition tunnel direction is parallel to the direction of the maximum horizontal principal compressive stress. However, the direction of the maximum horizontal stress could vary within 145±15° (SKB, 2009, p. 29) and the tunnel orientation could vary within 145±30° (SKB, 2010a, p. 56), implying that the tunnel orientation could deviate from the maximum horizontal stress orientation by up to 45°. The authors performed calculations using models 5–7 to explore the effects of such deviation. As Table 1 shows, models 6 and 7 predicted inelastic deformation on the floor and wall of the deposition tunnel and near the top of the deposition hole. Model 7 differs from model 6 in that the tensile strength was specified as a constant in model 6 but increased monotonically with plastic strain in model 7 (in an attempt to increase numerical stability of the model). Results from the two models show inelastic deformation, but the calculations did not proceed far enough in time to enable a determination of the magnitude and extent of inelastic deformation. The calculation terminated prematurely because of numerical instability at approximately 8 years for model 6 and approximately 13 years for model 7. Based on the model 7 result (see Figure A.2-11), the authors conclude that inelastic deformation could extend to a depth of at least 1 m below the tunnel floor and approximately 0.5 m into the tunnel wall for a tunnel orientation deviating by 45° from the orientation of the maximum horizontal principal stress.

Hydrological implication of the calculated inelastic deformation

The authors considered whether inelastic deformations could be represented using the stylized fracture models that SKB (2011, p. 333–335) used to estimate stress-induced changes in fracture aperture. However, the authors concluded based on the shape of the distribution of plastic strain magnitudes (e.g., Figure A.2-11) that a diffuse network of variously oriented fractures and microcracks could represent the deformations better than a single vertical or horizontal fracture. The authors are not aware of a reliable analytical approach for estimating the hydraulic conductivity of the zone of damaged rock represented by the inelastic deformation zone. However, experimental results reviewed by Bäckblom, (2008) and cited by SKB (2011, p. 160) suggest a hydraulic conductivity in the range of 10^{-8} – 10^{-6} m/s. The corresponding transmissivities could be determined using estimated EDZ dimensions.

Table 1: Summary of numerical models used to evaluate the mechanical behaviour of near-field host rock in the deposition area. The orientation of the maximum horizontal stress is assumed to be 145°.

Model number	Material property set	Material property modification	Deposition tunnel orientation	Inelastic deformation (rock damage)
1	Mean intact rock	None	145°	Did not occur
2	Mean intact rock	Minimum tensile strength	145°	Did not occur
3	Mean intact rock	Maximum Young's modulus and minimum tensile strength	145°	Did not occur
4	Mean rock mass	None	145°	Did not occur
5	Mean rock mass	None	167.5°	Did not occur
6	Mean rock mass	None	190°	Tunnel floor and wall.
7	Mean rock mass	Strain-hardened tensile strength	190°	Tunnel floor and wall. Deposition hole top
8 (glacial loading superimposed on stresses from case 5)	Mean rock mass	None	167.5°	Did not occur

3. The Consultants' overall assessment

Based on the evaluations documented in Section 2.3, the authors conclude that the SKB assessment of the occurrence of damaged rock zones in the disposal area, which SKB described in the SR-Site main report (SKB, 2011, p. 348) and implemented in the flow and transport model (SKB, 2011, Figure 13-13, p. 648), is supported by the SKB proposal to excavate the deposition tunnels using smooth blasting techniques. Furthermore, SKB will develop and implement procedures to control and inspect the drilling, charging, and ignition sequences and include the procedures in the monitoring and control programs for the underground openings to ensure reliable implementation of the smooth blasting technique.

Also, independent calculations that the authors performed indicate that the mechanical conditions in the disposal area are unlikely to result in additional rock damage if the disposal tunnels are oriented parallel to the direction of the maximum horizontal principal compressive stress. However, the current SKB proposed layout of the deposition tunnels includes a potential for the tunnel orientation to deviate enough from the preferred direction to set up mechanical conditions that could result in additional rock damage. If the tunnel layout includes the possibility for a large deviation of the tunnel orientation from the direction of the maximum horizontal stress (the authors' independent analysis indicates that a 45° deviation would be large enough to result in inelastic deformation), then the EDZ model configuration would need to be modified to account for potential stress-induced rock damage. However, if the allowable deviation of the tunnel orientation from the direction of the maximum horizontal stress is restricted to small values (the authors' independent analysis indicates that a 22.5° deviation would be small enough), then additional stress-induced damage would be unlikely and a modification of the EDZ configuration would not be necessary. The authors note that the uncertainty of ±15° in the orientation of the horizontal principal stress is included in any assessment of the tunnel orientation deviation from the stress orientation.

In addition to the information provided through this Technical Note, SSM has gathered rock damage assessments based on (1) spalling analysis, (2) fracture reactivation analysis, and (3) generalized inelastic deformation analysis. The first analysis focusses on rock damage at the excavation walls, whereas the second and third analyses focus on rock damage within the host rock interior. Therefore, synthesizing the results from the three analysis categories into a coherent set of information to be used to evaluate a rock damage assessment could be challenging.

4. References

Bäckblom G, 2008. Excavation damage and disturbance in crystalline rock – results from experiments and analyses. SKB TR-08-08, Swedish Nuclear Fuel and Waste Management Company (SKB).

Dassault Systèmes, 2012. ABAQUS® User Manual (version 6.12). SIMULIA, a division of Dassault Systèmes, Providence, Rhode Island.

Diederichs M S. 2007. The 2003 Canadian geotechnical colloquium: Mechanistic interpretation and practical application of damage and spalling prediction criteria for deep tunnelling. *Canadian Geotechnical Journal* 44: 1082–1116.

Ericsson L O, Brinkhoff P, Gustafson G, Kvartsberg S, 2009. Hydraulic features of the Excavation Disturbed Zone. Laboratory investigations of samples taken from the Q- and S-tunnels at Äspö HRL. SKB R-09-45, Swedish Nuclear Fuel and Waste Management Company (SKB).

Hökmark H, Lönnqvist M, Fälth B, 2010. THM-issues in repository rock. Thermal, mechanical, thermo-mechanical and hydromechanical evolution of the rock at the Forsmark and Laxemar sites. SKB TR-10-23, Swedish Nuclear Fuel and Waste Management Company (SKB).

Olsson M, Niklasson B, Wilson L, Andersson C, Christiansson R, 2004. Äspö HRL. Experiences of blasting of the TASQ tunnel. SKB R-04-73, Swedish Nuclear Fuel and Waste Management Company (SKB).

Olsson M, Markström I, Pettersson A, Sträng M, 2009. Examination of the Excavation Damaged Zone in the TASS tunnel, Äspö HRL. SKB R-09-39, Swedish Nuclear Fuel and Waste Management Company (SKB).

Ord A, 1991. Deformation of rock: A pressure-sensitive, dilatant material. *Pure and Applied Geophysics* **137**: 337–366.

SKB, 2009. Underground design Forsmark. Layout D2. SKB TR-08-116, Swedish Nuclear Fuel and Waste Management Company (SKB).

SKB, 2010a. Design, construction and initial state of the underground openings. SKB TR-10-18, Swedish Nuclear Fuel and Waste Management Company (SKB).

SKB, 2010b. Data report for the safety assessment SR-Site. SKB TR-10-52, Swedish Nuclear Fuel and Waste Management Company (SKB).

SKB, 2011. Long-term safety for the final repository at Forsmark: Main report of the SR-Site project (3 volumes). SKB TR-11-01, Swedish Nuclear Fuel and Waste Management Company (SKB).

APPENDIX 1

Coverage of SKB reports

Table A.1-1. Coverage of SKB reports reviewed by the authors.

Reviewed report	Reviewed sections	Comments
SKB TR-11-01, Long-term safety for the final repository for spent nuclear fuel at Forsmark. Main report of the SR-Site project, Volume I	4, 5, 6, 7	
SKB TR-11-01, Long-term safety for the final repository for spent nuclear fuel at Forsmark. Main report of the SR-Site project, Volume II	10	
SKB TR-11-01, Long-term safety for the final repository for spent nuclear fuel at Forsmark. Main report of the SR-Site project, Volume III		
SKB TR-10-52, Data report for the safety assessment	5, 6	
SKB TR-08-116, Underground design Forsmark. Layout D2	3, 4	
SKB TR-10-23, THM-issues in repository rock. Thermal, mechanical, thermo-mechanical and hydromechanical evolution of the rock at the Forsmark and Laxemar sites	2, 4, 5, 6, 7	
SKB TR-00-05, Thermo-mechanical effects from a KBS-3 type repository. Performance of pillars between repository tunnels	2, 3	
SKB R-07-31, Rock Mechanics Forsmark. Site descriptive modelling Forsmark stage 2.2	3, 5, 6, 7	

Consultants' independent calculations

A.2.1. Introduction

This appendix describes independent ABAQUS calculations that were conducted to support the review of *Rock Mechanics – Confidence of SKB's models for predicting the occurrence of a damage zone around the excavations*. The evaluations are based on an ABAQUS (Dassault Systèmes, 2012) thermal-mechanical analysis performed using a three-dimensional quarter-symmetry model similar to the model described by Hakami and Olofsson (2000), but with deposition tunnel and hole dimensions and spacing as specified for the Layout D2 design in SKB (2009), Figure A.2-1, and Table A.2-1.

A.2.2. Model Description

The modelling effort uses two separate ABAQUS analyses. First, an uncoupled heat transfer analysis is used to determine the temperature distribution in the model domain for use in the subsequent stress analysis. For the heat transfer analysis, the model extends from ground surface (elevation 0 m) to a depth of 1,000 m. The initial temperature distribution as a function of depth was interpolated from data in Hökmark et al. (2010, p. 40, Table 4-4) as follows

$$Temperature = 0.0115 \times Depth + 5.88 \qquad \text{(Eqn. 1)}$$

and gives a value of 11.2 °C at a depth of 460 m. The temperature load as a function of time (Figure A.2-2) at the deposition hole wall was interpolated from data in Hökmark et al. (2010).

The stress analysis portion of the ABAQUS calculation imports the temperature history from the prior heat transfer analysis. The stress analysis model extends from a depth of −410 m to ~−518 m (Figure A.2-1). In addition to the temperature load, the stress analysis includes the specified *in situ* stress conditions, swelling pressures for the tunnel floor/wall/side and deposition hole wall/floor, glacial loading (stress) history, and pore pressure history. The stress analysis covers a time period of 100,000 years, which includes one glacial loading/unloading cycle. The first glacial cycle starts at 55,000 years in the ABAQUS model, with the peak in glacial loading occurring at 62,000 years.

The *in situ* stress at a depth of 460 m was interpolated from data presented in SKB (2010) based on data from Glamheden et al. (2007): (i) the maximum principal stress is horizontal ($\sigma_1 = \sigma_H$) and parallel to the deposition tunnel with a magnitude of 40.1 MPa; (ii) the intermediate principal stress is horizontal ($\sigma_2 = \sigma_h$) and perpendicular to the deposition tunnel with a magnitude of 22.1 MPa; and (iii) the minimum principal stress is vertical ($\sigma_3 = \sigma_V$) with a magnitude of 12.2 MPa. In addition to this standard stress state configuration, models were considered in which

the horizontal stresses were rotated 22.5°, 45°, and 90° (i.e., σ_H oriented perpendicular to the tunnel).

Based on the site hydraulic gradient and resaturation time described in SKB (2011, p. 368–373), the pre-glacial pore pressure is specified to be 0 MPa until 900 years, increasing to 5 MPa by 1,000 years, and then maintaining a constant value at 5 MPa until impacted by the glacial loading cycle. Based on Hökmark et al. (2010), the glacial cycle adds an additional pore pressure of 98% of the glacially induced vertical load. The glacially induced pore pressure component (in addition to the 5 MPa pre-glacial value) begins increasing at 55,000 years, reaches a maximum value of ~17.64 MPa (i.e., 98% of the 18 MPa vertical load) at 62,000 years, decreases to 0 MPa at 65,000 years, begins increasing again at 89,000 years, and reaches ~24.5 MPa (i.e., 98% of the 25 MPa vertical load) at 100,000 years (Figure A.2-3).

For the ABAQUS models, the internal pressure in the tunnel and deposition hole equals the sum of the swelling pressure (of backfill for the tunnel and buffer for the deposition hole) and the groundwater pressure and follows the time evolution of groundwater pressure. As such, the internal pressures are set to 0 MPa from the beginning of the stress analysis until 900 years. The values increase to 12 MPa for the deposition hole (7 MPa swelling plus 5 MPa background pore pressure) and 5.5 MPa for the tunnel (0.5 MPa swelling plus 5 MPa background pore pressure) from 900 to 1000 years. The values of swelling pressure were based on SKB (2011, p. 373–379) information. Once the glacial loading influence on pore pressure begins, the internal pressures are modified with the new pore pressure component (Figure A.2-4).

The stress history due to glacial loading is taken from Hökmark et al. (2010) with some simplifications (Figure A.2-5). The first glacial maximum coincides with 62,000 years in the ABAQUS model (12,000 years from beginning of first glacial cycle). The glacially induced vertical stress component (on top of the 12.2 MPa initial value) begins increasing from 0 MPa at 55,000 years, reaches a maximum of ~18 MPa at 62,000 years, and drops back to 0 MPa at 65,000 years. The glacially induced vertical stress component begins increasing again at 90,000 years (beginning of next glacial load) and reaches a value of ~25 MPa at 100,000 years. The glacially induced tunnel parallel stress component (on top of the 40.1 MPa initial value) begins increasing from 0 MPa at 55,000 years, reaches a maximum of ~15 MPa at 62,000 years, drops to ~5.5 MPa at 65,000 years, is 0 MPa at 89,000 years, and ramps back up to ~24 MPa at 100,000 years. The glacially induced tunnel perpendicular stress component (on top of the initial value of 22.1 MPa) begins increasing from 0 MPa at 55,000 years, reaches a maximum of ~15 MPa at 62,000 years, drops to ~7 MPa at 65,000 years, is 0 MPa at 89,000 years, and ramps back up to ~24 MPa at 100,000 years.

Rock strength and stiffness were modelled using an elastic-plastic constitutive model in ABAQUS based on linear elasticity with the Mohr-Coulomb yield criterion. The model captures both the elastic and inelastic strains if the loading conditions satisfy the yield criteria. Two primary material property sets were considered, one representing intact rock conditions (Table A.2-2) and one representing rock mass conditions (Table A.2-3). As stated in Tables A.2-2 and A.2-3, the value of Young's modulus is 70±8 GPa for the intact rock material property set and 72 GPa for the rock mass material property based on SKB information cited in the tables. However, the fact that the mean value for the rock mass is slightly greater than the mean value for the intact rock should not cause any concern. Either

of the mean values could be adjusted by examining the SKB data and the calculations used to determine the values. Moreover, a sensitivity analysis of the intact rock model indicates that the calculated response is not affected by changing the Young's modulus from the mean value of 70 GPa to the maximum value of 78 GPa. The ABAQUS constitutive model also requires specifying the dilation angle, which is not reported in the available SKB documents. Based on the reviewers' past experience with this type of analysis, the dilation angle was set to 10% of the friction angle. As discussed below, some additional variations in material properties were also considered on a case-by-case basis.

A.2.3. Model Results

As discussed above, the ABAQUS calculations were performed in two analysis steps. The initial heat transfer step served only to provide the temperature distribution over time throughout the model domain for the stress analysis step. To confirm that the heat transfer step correctly calculated the temperature field and that the stress analysis step correctly imported the temperature field, the temperature versus time histories were extracted from a node on the deposition hole wall (Figure A.2-6).

The suite of ABAQUS calculations (Table A.2-4) can be subdivided into broad groups, which we refer to as the typical model case and the pessimistic model case. The calculations under the typical model case use the intact rock material properties (or slight variations thereof), whereas calculations under the pessimistic model case employ the rock mass material properties (or slight variations thereof).

A.2.3.1. Intact Rock Properties Model Results

Model 1 employs the intact rock material properties specified in Table A.2-2 as well as all the loading conditions described above. Although the applied loads lead to variable stress development both spatially and temporally, the model does not predict any inelastic strain occurring in the model domain (Figure A.2-7). Model 2 was identical to model 1, but with a reduced tensile strength of 7.9 MPa, representing the minimum value reported by Glamheden et al. (2007, Table 3-3). This value of tensile strength contrasts with the mean value of 11.1 MPa used in Model 1. No inelastic strain is predicted in model 2. As a further test, model 3 was constructed with a Young's modulus of 78 GPa, representing the maximum value reported by SKB (2010, Table 6-55), but otherwise identical to model 2. This higher Young's modulus value was selected to maximize the impact of the thermal loading. As with models 1 and 2, model 3 does not predict the development of any inelastic strain in response to the applied loading conditions.

Results of the ABAQUS calculations using intact rock properties, even allowing for a reduced tensile strength and an increased stiffness, suggest that inelastic strain (damage) around the deposition holes and tunnels is unlikely.

A.2.3.2. Rock Mass Properties Model Results

In order to consider more pessimistic starting conditions, a series of models was constructed that employed the rock mass material properties (Table A.2-3). Model 4 uses all the loading conditions described above. Despite the reduced rock strength (smaller friction angle, unconfined compressive strength, and tensile strength) of the rock mass properties, model 4 does not indicate any inelastic strain development

(Figure A.2-8). To assess the impact of tunnel orientation uncertainty, model 5 was constructed with the tunnel orientation rotated 22.5° relative to the default case of 145° (new orientation 167.5°). Despite the tunnel reorientation, model 5 does not predict any inelastic strain development. Model 6 was constructed with the tunnel orientation rotated 45° (new orientation 190°). Results for model 6 indicate that the 45° tunnel rotation leads to early development of tensile plastic strain that is focused primarily in the deposition tunnel floor and lower wall with some localization near the top of the deposition hole (Figure A.2-9). The inelastic strains extend into the rock mass ~1 m. Because of the early plastic strain development, model 6 did not progress beyond ~8 years. In an effort to achieve a longer model analysis time, model 7 was constructed by modifying the material property description to allow for a small amount of tensile strain hardening. The initial tensile strength of 2.4 MPa was increased to 3.6 MPa at a strain of 10^{-5} and then to 4.8 MPa at a strain of 10^{-4}. Model 7 progressed to ~13 years and results indicate that even with the tensile strength hardening, inelastic strain will develop during the first decade or so after waste emplacement (Figures A.2-10 and A.2-11). The early strain development is still tensile; compressive plastic strains are also well-developed in the floor of the deposition tunnel by ~13 years. To confirm that glacial loading would not induce inelastic strain, model 8 was constructed using model 5 as the base. The stress state at ~50,000 years from model 5 was used as the initial stress state for model 8. Then the glacial loading was applied as in other models. Model results indicate that the glacially induced stresses do not induce inelastic strain.

Results of the ABAQUS calculations using rock mass properties and the default stress orientations (maximum principal stress parallel to the deposition tunnels) suggest that inelastic strain (damage) around the deposition holes and tunnels is unlikely. Rotation of the maximum tunnel orientation as much as 22.5° from the default value of 145° does not appear to affect this result. However, the ABAQUS calculations do suggest the potential for damage near the tunnel wall and floor, as well as the deposition hole wall, if the tunnel orientation is rotated 45° or more compared to the default value (Figure A.2-11).

Table A.2-1: ABAQUS model dimensions.

Dimension	Value	Reference
Deposition tunnel center-to-center spacing (m)	40	SKB, 2009, p. 29
Deposition hole center-to-center spacing (m)	6	SKB, 2009, p. 29
Deposition hole depth (m)	8.2	SKB, 2009, A8, p. 110
Deposition hole diameter (m)	1.75	SKB, 2009, A8, p. 110
Deposition hole radius (m)	0.875	SKB, 2009, A8, p. 110
Deposition tunnel floor at elevation (m)	-460	Hökmark et al., 2010, p. 34
Deposition tunnel vertical wall height (m)	3.6	SKB, 2009, A8, p. 110
Deposition tunnel center wall height (m)	4.8	SKB, 2009, A8, p. 110

Table A.2-2: Intact rock material properties

Dimension	Value	Reference
Density [kg/m^3]	2700	Hökmark et al., 2010, p. 41, Table 4-5
Young's modulus [GPa]	70 ± 8	Hökmark et al., 2010, p. 41, Table 4-5
Poisson's ratio	0.24	Hökmark et al., 2010, p. 41, Table 4-5
Friction angle [°]	60	Glamheden et al., 2007, p. 43, Table 3-5
Cohesion [MPa]	30.28	n.a.*
Unconfined compressive strength [MPa]	226	Hökmark et al., 2010, p. 41, Table 4-5
Tensile strength [MPa]	11.1 ± 3.2	Glamheden et al., 2007, p. 41, Table 3-3
Thermal conductivity [J/(s•m•K)]	3.57	Hökmark et al., 2010, p. 41, Table 4-5
Thermal expansivity [K^{-1}]	7.7e-6	Hökmark et al., 2010, p. 41, Table 4-5
Specific heat [MJ/(m^3•K)]	2.06	Hökmark et al., 2010, p. 41, Table 4-5

*Cohesion calculated from friction angle and unconfined compressive strength.

Table A.2-3: Rock mass material properties.

Dimension	Value	Reference
Density [kg/m^3]	2700	Hökmark et al., 2010, p. 41, Table 4-5
Young's modulus [GPa]	72	Glamheden et al., 2007, p. 82, Table 5-2
Poisson's ratio	0.23	Glamheden et al., 2007, p. 82, Table 5-2
Friction angle [°]	50	Glamheden et al., 2007, p. 82, Table 5-2
Cohesion [MPa]	27	Glamheden et al., 2007, p. 82, Table 5-2
Unconfined compressive strength [MPa]	146	Glamheden et al., 2007, p. 82, Table 5-2
Tensile strength [MPa]	2.4	Glamheden et al., 2007, p. 82, Table 5-2
Thermal conductivity [J/(s•m•K)]	3.57	Hökmark et al., 2010, p. 41, Table 4-5
Thermal expansivity [K^{-1}]	7.7e-6	Hökmark et al., 2010, p. 41, Table 4-5
Specific heat [MJ/(m^3•K)]	2.06	Hökmark et al., 2010, p. 41, Table 4-5

Table A.2-4: Summary of ABAQUS models.

Model	Material Property Set	Material Property Modification	Tunnel Orientation
1	Mean intact	n.a.	145°
2	Mean intact	Tensile strength decreased	145°
3	Mean intact	Young's modulus increased	145°
4	Rock Mass	n.a.	145°
5	Rock Mass	n.a.	167.5°
6	Rock Mass	n.a.	190°
7	Rock Mass	Tensile strength hardening	190°
8 (glacial loading superimposed on stresses from case 5)	Rock Mass	n.a.	167.5°

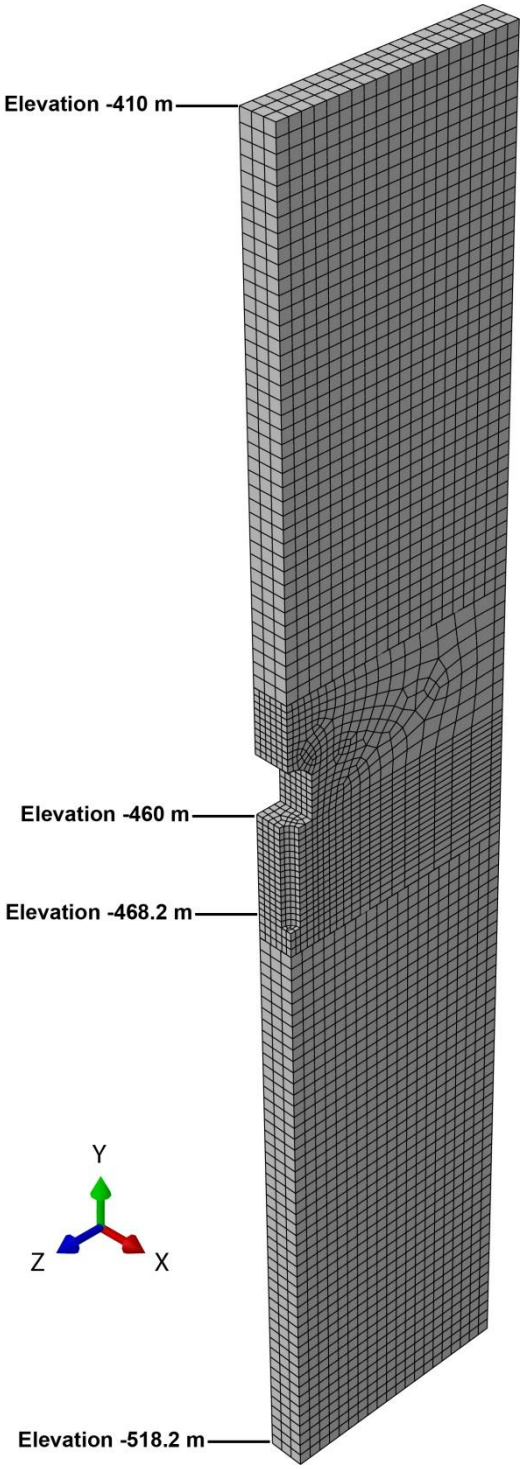

Figure A.2-1. Illustration of basic model geometry for stress analysis portion of the ABAQUS calculations. Model domain for heat transfer portion extends upwards to the ground surface (elevation 0 m) and downward to a depth of 1,000 m. In the ABAQUS coordinate reference frame, X is parallel to the deposition tunnel, Z is perpendicular to the deposition tunnel, and Y is vertical (positive upwards).

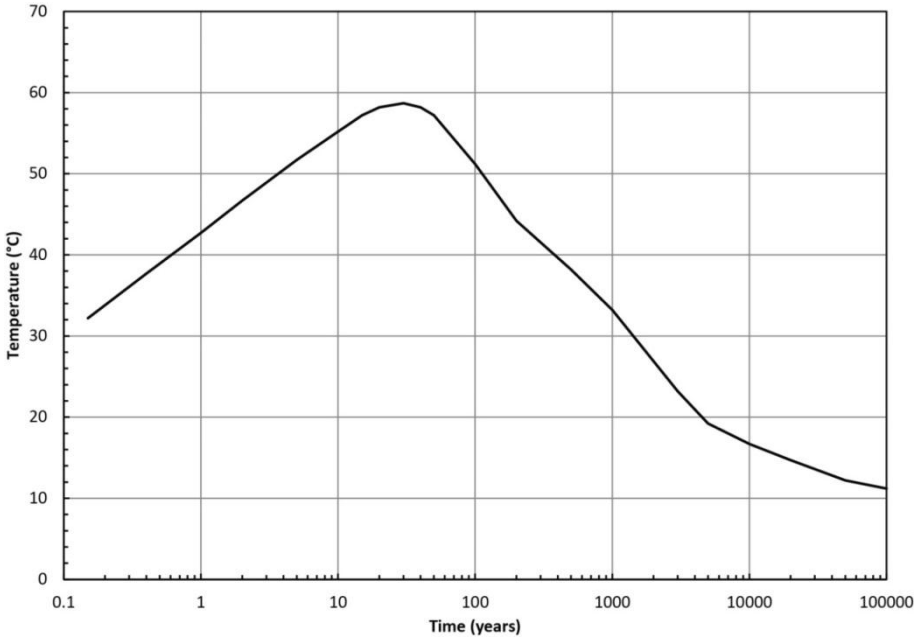

Figure A.2-2. Temperature versus time function applied at deposition hole wall during heat transfer analysis portion of ABAQUS calculations.

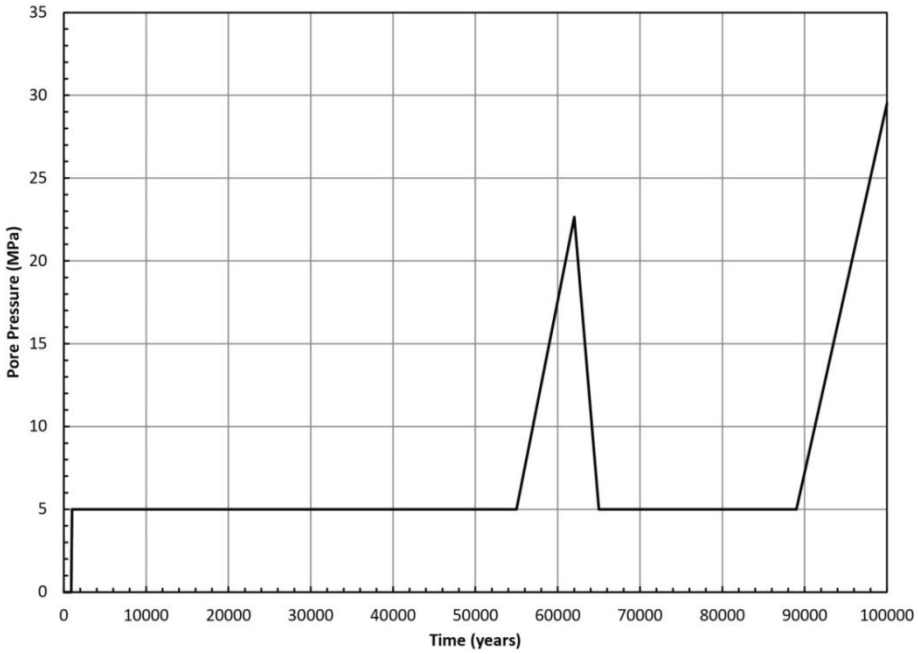

Figure A.2-3. Pore pressure versus time function applied to model domain during stress analysis portion of ABAQUS calculations.

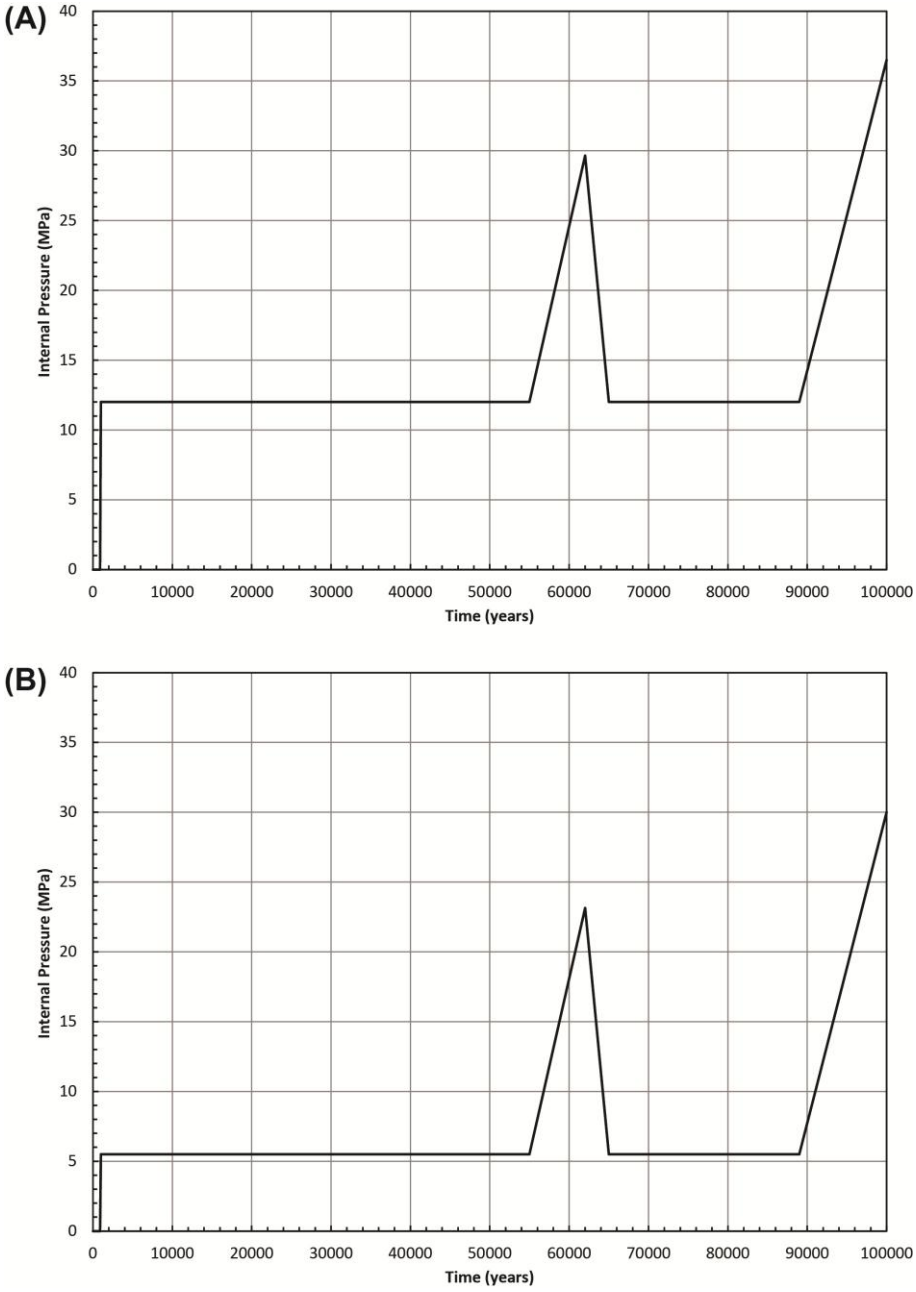

Figure A.2-4. Internal pressure (swelling pressure + pore pressure) versus time function applied to (A) deposition hole wall and floor and (B) tunnel roof, wall, and floor during stress analysis portion of ABAQUS calculations.

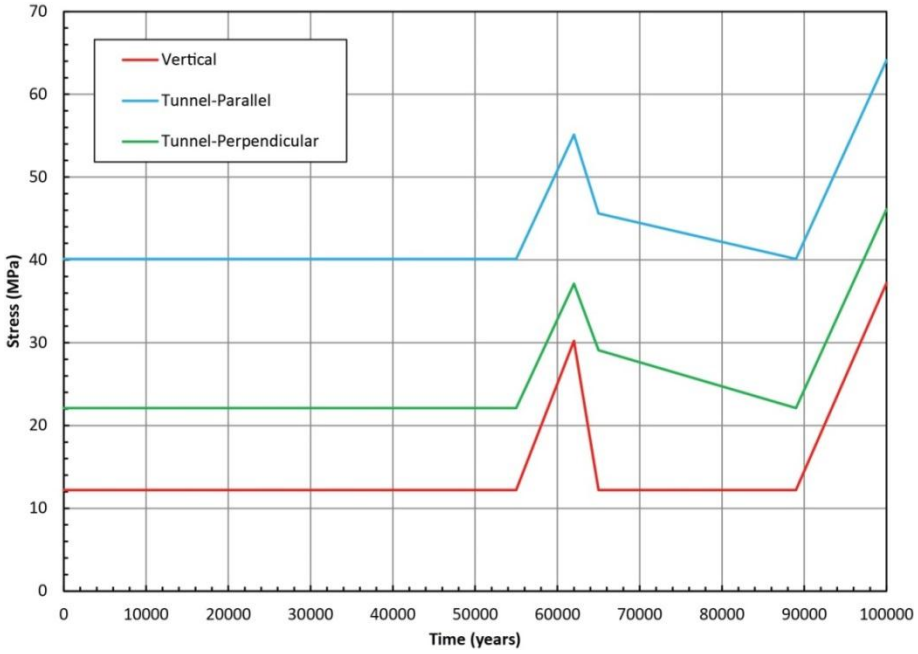

Figure A.2-5. Stress magnitudes versus time function applied to model domain during stress analysis portion of ABAQUS calculations. Note that stresses are shown here with compression positive, although ABAQUS internally treats compression as negative.

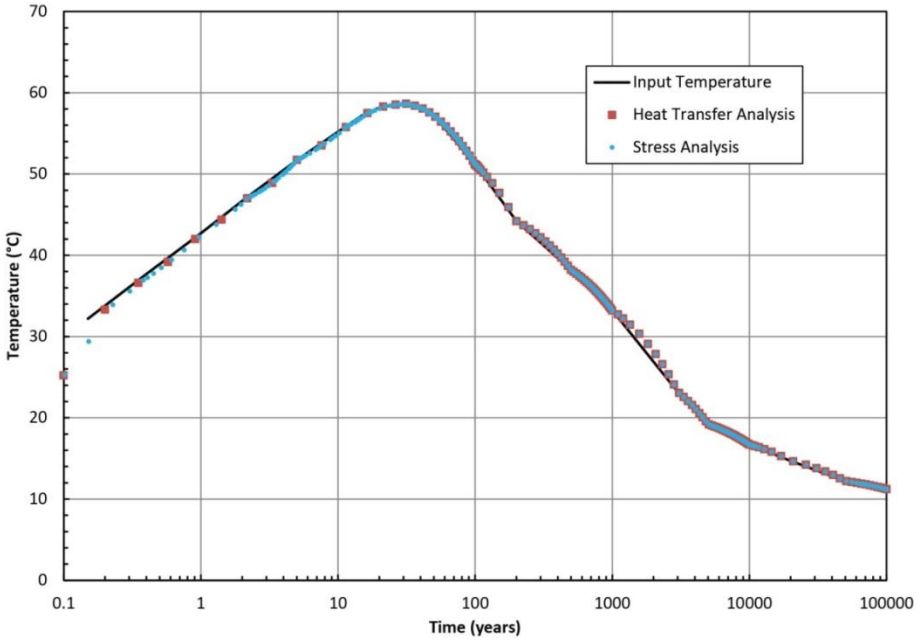

Figure A.2-6. Comparison of input temperature history at the deposition hole wall, temperature history calculated in the heat transfer analysis step, and the temperature imported into stress analysis transfer step.

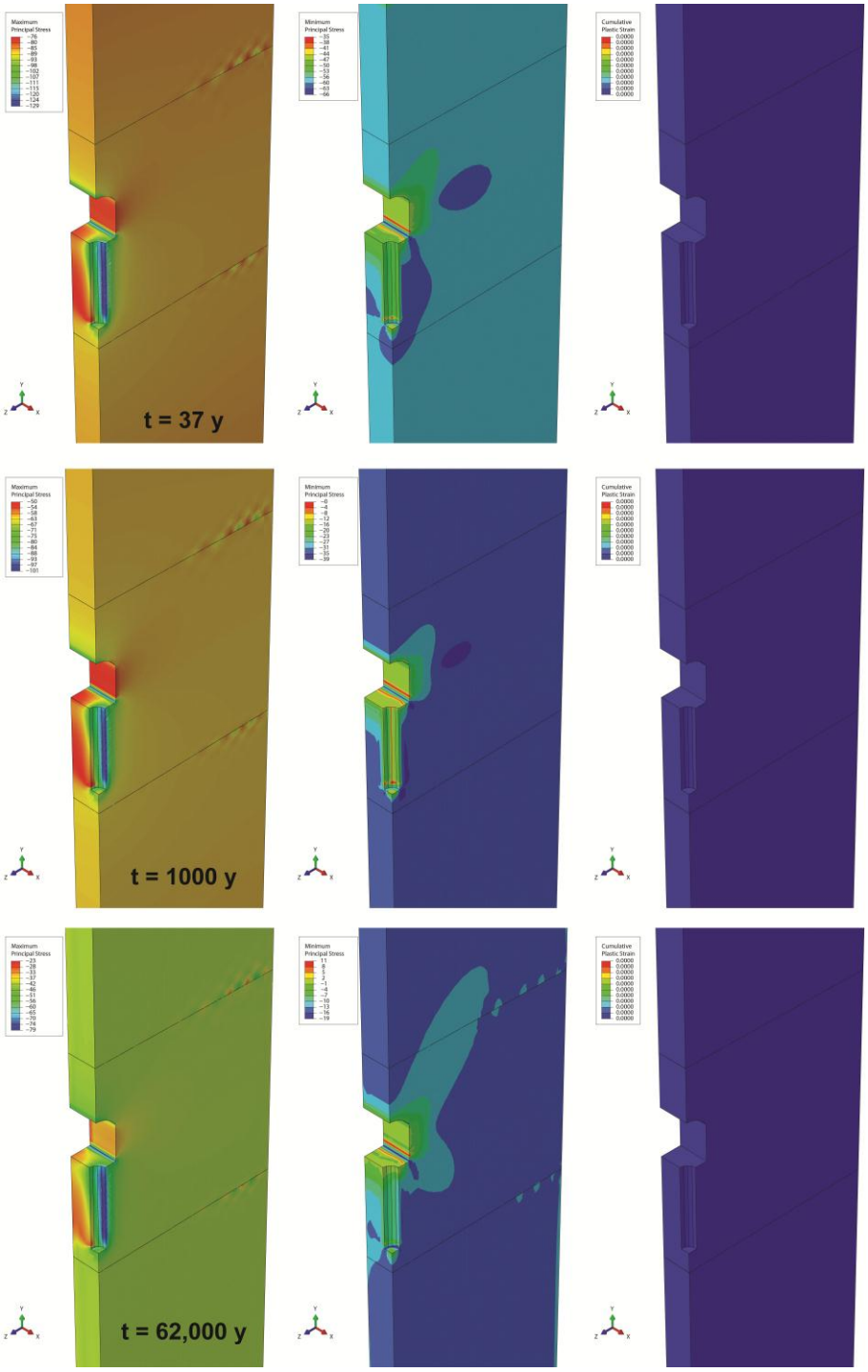

Figure A.2-7. Model 1 results (mean intact material property set; maximum principal stress is parallel to the deposition tunnel) showing magnitudes of maximum principal stress (left column), minimum principal stress (center column), and cumulative plastic strain (right column). Results are shown for peak thermal pulse at ~37 years (top row), achievement of full saturation at 1000 years (middle row), and glacial loading peak at ~62,000 years (bottom row). Stresses are in MPa.

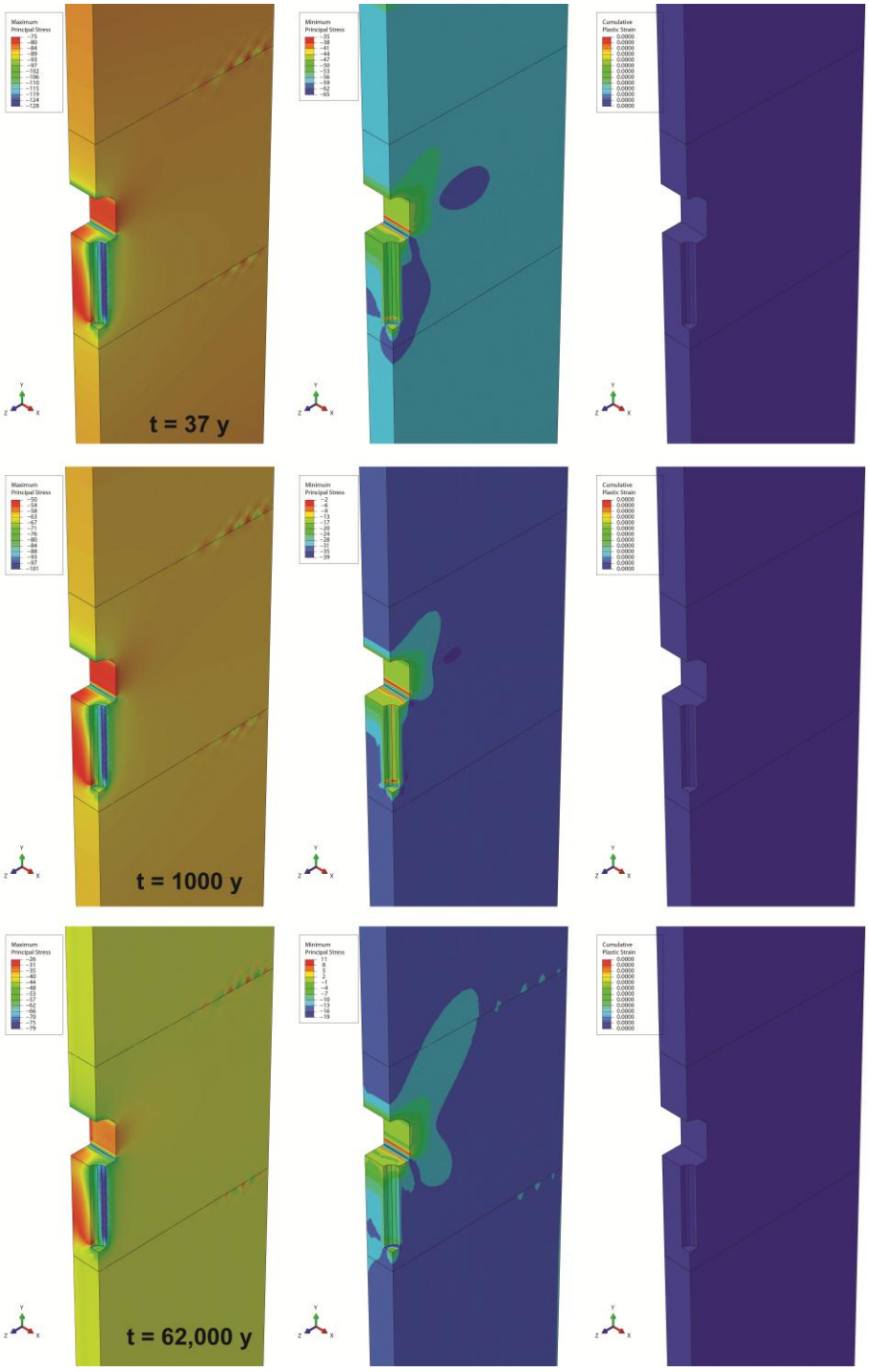

Figure A.2-8. Model 4 (rock mass material property set; maximum principal stress is parallel to the deposition tunnel) results showing magnitudes of maximum principal stress (left column), minimum principal stress (center column), and cumulative plastic strain (right column). Results are shown for peak thermal pulse at ~37 years (top row), achievement of full saturation at 1,000 years (middle row), and glacial loading peak at ~62,000 years (bottom row). Stresses are in MPa.

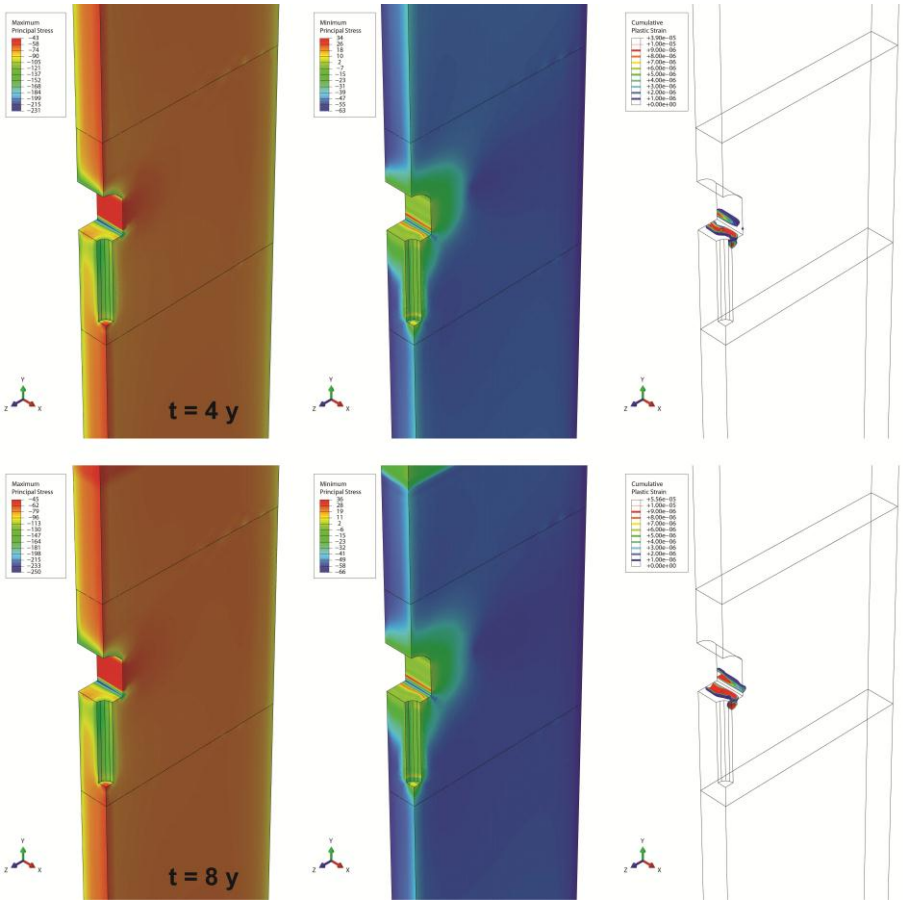

Figure A.2-9. Model 6 results (rock mass material property set; maximum principal stress is 45° to the deposition tunnel) showing magnitudes of maximum principal stress (left column), minimum principal stress (center column), and cumulative plastic strain (right column). Results are shown at ~4 years (top row) and at ~8 years (bottom row). Stresses are in MPa. Cumulative plastic strain is due to tensile failure.

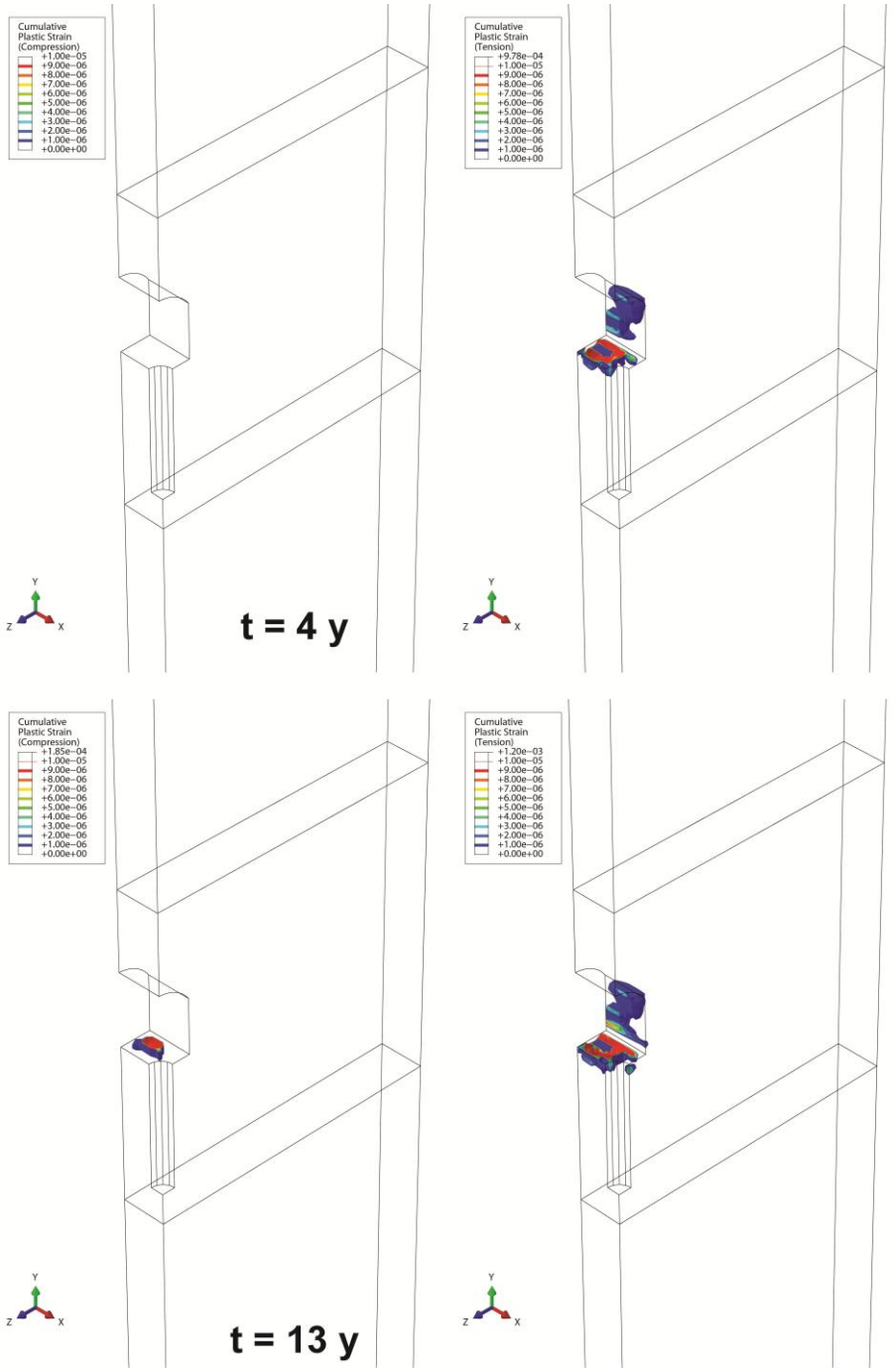

Figure A.2-10. Model 7 results (rock mass material property set; maximum principal stress is 45° to the deposition tunnel) showing magnitudes of cumulative plastic strain due to compressive failure (left column) and tensile failure (right column). Results are shown at ~4 years (top row) and at ~13 years (bottom row).

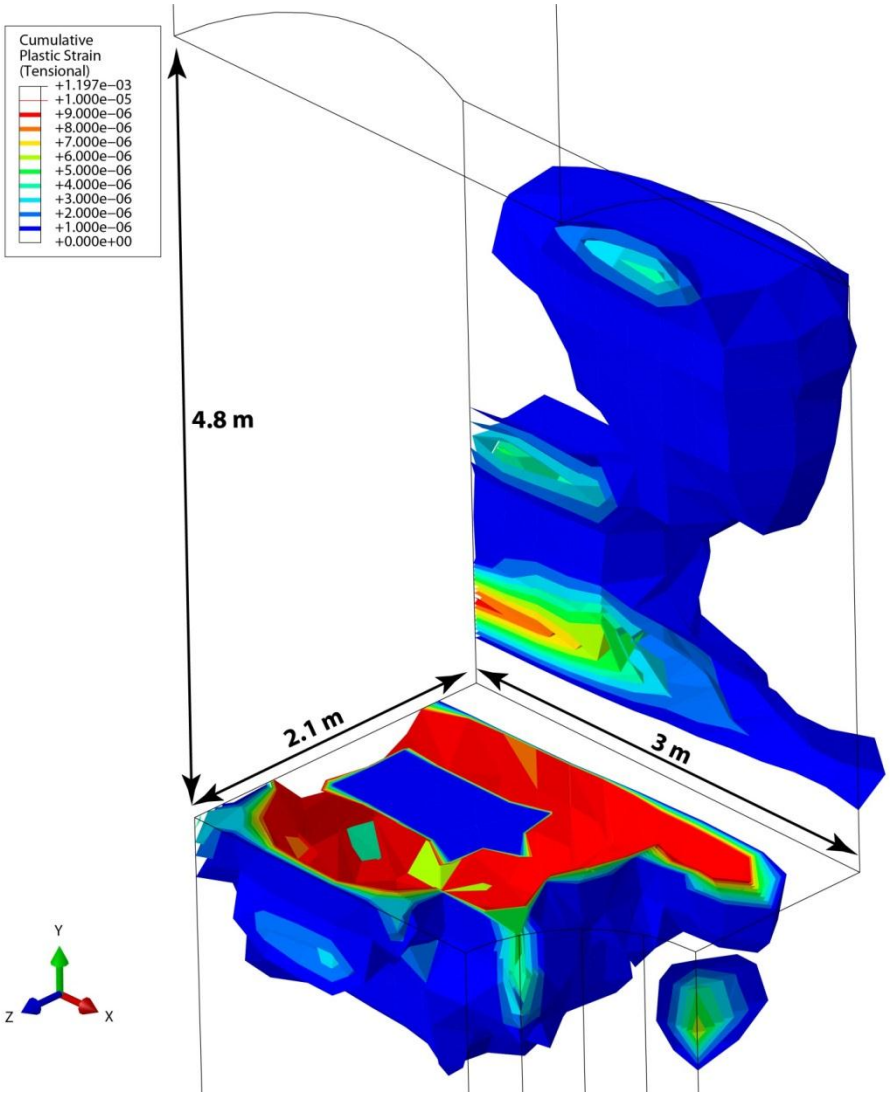

Figure A.2-11. Enlarged view of Model 7 results showing magnitude of cumulative plastic strain due to tensile failure at ~13 years.

A.2.4. References

Dassault Systèmes, 2012. ABAQUS® User Manual (version 6.12). SIMULIA, a division of Dassault Systèmes, Providence, Rhode Island.

Glamheden R, Fredriksson A, Röshoff K, Karlsson J, Hakami H, Christiansson R, 2007. Rock Mechanics Forsmark. Site descriptive modelling Forsmark stage 2.2. SKB R-07-31, Swedish Nuclear Fuel and Waste Management Company (SKB).

Hakami E, Olofsson S-O, 2000. Thermo-mechanical effects from a KBS-3 type repository. Performance of pillars between repository tunnels. SKB TR-00-05, Swedish Nuclear Fuel and Waste Management Company (SKB).

Hökmark H, Lönnqvist M, Fälth B, 2010. THM-issues in repository rock. Thermal, mechanical, thermo-mechanical and hydromechanical evolution of the rock at the Forsmark and Laxemar sites. SKB TR-10-23, Swedish Nuclear Fuel and Waste Management Company (SKB).

SKB, 2009. Underground design Forsmark. Layout D2. SKB R-08-116, Swedish Nuclear Fuel and Waste Management Company (SKB).

SKB, 2010. Data report for the safety assessment SR-Site. SKB TR-10-52, Swedish Nuclear Fuel and Waste Management Company (SKB).

SKB, 2011. Long-term safety for the final repository at Forsmark: Main report of the SR-Site project (3 volumes). SKB TR-11-01, Swedish Nuclear Fuel and Waste Management Company (SKB).

2013:35

The Swedish Radiation Safety Authority has a comprehensive responsibility to ensure that society is safe from the effects of radiation. The Authority works to achieve radiation safety in a number of areas: nuclear power, medical care as well as commercial products and services. The Authority also works to achieve protection from natural radiation and to increase the level of radiation safety internationally.

The Swedish Radiation Safety Authority works proactively and preventively to protect people and the environment from the harmful effects of radiation, now and in the future. The Authority issues regulations and supervises compliance, while also supporting research, providing training and information, and issuing advice. Often, activities involving radiation require licences issued by the Authority. The Swedish Radiation Safety Authority maintains emergency preparedness around the clock with the aim of limiting the aftermath of radiation accidents and the unintentional spreading of radioactive substances. The Authority participates in international co-operation in order to promote radiation safety and finances projects aiming to raise the level of radiation safety in certain Eastern European countries.

The Authority reports to the Ministry of the Environment and has around 270 employees with competencies in the fields of engineering, natural and behavioural sciences, law, economics and communications. We have received quality, environmental and working environment certification.

Strålsäkerhetsmyndigheten
Swedish Radiation Safety Authority

SE-171 16 Stockholm
Solna strandväg 96

Tel: +46 8 799 40 00
Fax: +46 8 799 40 10

E-mail: registrator@ssm.se
Web: stralsakerhetsmyndigheten.se